Field-theoretical renormalization group for a flat two-dimensional Fermi surface

H. Freire, E. Corrêa and A. Ferraz
Laboratório de Supercondutividade,
Centro Internacional de Física da Matéria Condensada,
Universidade de Brasília - Brasília, Brazil
(Dated: February 2, 2008)

We implement an explicit two-loop calculation of the coupling functions and the self-energy of interacting fermions with a two-dimensional flat Fermi surface in the framework of the field theoretical renormalization group (RG) approach. Throughout the calculation both the Fermi surface and the Fermi velocity are assumed to be fixed and unaffected by interactions. We show that in two dimensions, in a weak coupling regime, there is no significant change in the RG flow compared to the well-known one-loop results available in the literature. However, if we extrapolate the flow to a moderate coupling regime there are interesting new features associated with an anisotropic suppression of the quasiparticle weight Z along the Fermi surface, and the vanishing of the renormalized coupling functions for several choices of the external momenta.

PACS numbers: 71.10.Hf, 71.10.Pm, 71.27.+a

I. INTRODUCTION

A better understanding of the physical properties of highly interacting electrons in two spatial dimensions (2D) is believed to be central for high-Tc superconductivity. Soon after the discovery of the high-Tc superconductors, Anderson[1] suggested that a strongly interacting 2D electron gas should resemble a 1D Luttinger liquid state. This question remains unresolved to this date. Thanks to the high precision angular resolved photoemission experiments performed in a variety of materials[2], we know, at present, important facts concerning the Fermi surface (FS) of the cuprates. The FS of underdoped and optimally doped Bi2212 and YBaCuO compounds contains both flat and curved sectors[3]. As a result, they are nearly perfectly nested along certain directions in momentum space. As is well-known, whenever there is a flat FS, the corresponding one-electron dispersion law resembles a 1D dispersion.

The cuprates are Mott insulators at half-filling which become metallic at very low doping[4]. At half-filling, Hubbard-like models have a square shape FS imposed by electron-hole symmetry. The FS changes as we vary the filling factor and, as soon as it is lightly doped, it acquires non-zero curvature sectors in k-space. However, in the immediate vicinity of half-filling, there are, at most, isolated curved spots in momentum space. Consequently, in a first analysis, one may neglect their presence altogether. Following this scheme, several workers investigated the properties of a 2D electron gas in the presence of a totally flat FS[5,6,7,8,9]. In their approaches, the FS is always kept fixed and never deviates from its original flat form. Besides that, their results conflict with each other. Conventional perturbation theory calculations[5], parquet method results[6], as well as one-loop perturbative RG calculations[7] indicate that, for repulsive interactions, there is never a Luttinger liquid state in 2D. For the repulsive Hubbard interaction, the one-loop calculations indicate that the antiferromagnetic spin density wave is the dominant instability in two dimensions. In contrast, applying bosonization methods, Luther was able to map the square FS onto two sets of perpendicular chains[8]. As a result of that, the corresponding electron correlation functions become sums of power law terms with exponents only differing in form from those of a Luttinger liquid[9]. Very recently, Rivasseau and collaborators using a mathematically rigorous renormalization group analysis[10] proved that, at finite temperatures, the half-filled Hubbard model in two dimensions with a perfectly square Fermi surface is indeed a Luttinger liquid apart from logarithmic corrections. That result adds new elements to the possible existence of a Luttinger liquid phase in two dimensions.

We report in this work a two-loop field theoretical RG calculation for the electron gas in the presence of the same flat FS model as used by Zheleznyak *et al.*[6]. Experimentally, such a FS was observed quite recently in an ARPES experiment performed in $La_{2-x}Sr_xCuO_{4-\delta}$ (LSCO) thin epitaxial film under strain[11]. On the theoretical side, all one-loop RG calculations presented so far for a flat 2D Fermi surface indicate a flow to a strong coupling regime. One should therefore check if a two-loop calculation changes that result or not. Besides, there have been recent works addressing the renormalization of the quasiparticle weight Z due to interactions[12,13]. Those works are not totally consistent since they ignore the feedback produced by Z in the RG equation for the coupling functions. We show that, as long as we restrict ourselves to the weak coupling regime, Z is only altered slightly from its unity value. As a result, in that limit the RG coupling flows are not severely modified by Z. In contrast, if we consider moderate couplings, there are substantial changes produced in the RG flow as opposed to the one-loop case, and Z indeed goes to zero in this region of coupling space.

In our analysis, we assume that the FS and the Fermi velocity v_F are not renormalized by the interactions. In a later work, we show how the renormalization of both v_F

and the FS may affect our results. The novel aspect of our work, apart from using a field theoretical RG approach to deal with a 2D fermionic problem, is the fact that we explicitly calculate all the two-loop diagrams for the self-energy and the renormalized coupling functions, taking full account of the variation of the momenta of the counterterms along the FS. As a result, we are able to calculate the nonleading logarithmic contributions originated by the so-called nonparquet diagrams and the self-energy corrections which lead to a momentum dependent quasiparticle weight $Z(\mathbf{p})$. To our knowledge, it is the first time that such a systematic and detailed two-loop calculation in two dimensions is presented in the context of the fermionic RG approach. For simplicity, and to make easier the comparison with other RG results, we use the so-called "g-ology" notation throughout this work. To reduce the number of accounted diagrams, we limit ourselves to backscattering and forward scattering processes only. The Umklapp scattering processes will not be considered since they only occur when the distance between the parallel FS patches is equal to π. We intend to include these contributions in a later publication.

Since the fermionic field theoretical RG is not widely known among condensed matter physicists we present the method at length and in full detail. We begin by presenting our Lagrangian model and the reasons why we need to apply the renormalization method in the first place for the flat FS. We calculate next the one-particle irreducible vertex functions associated with both forward and backscattering processes in one-loop order. We derive the RG equations for the renormalized coupling functions and show how they flow to strong coupling in agreement with the parquet and the other one-loop RG approaches. We then move on to calculate the self-energy in two-loop order. Using the renormalization theory we determine the quasiparticle weight Z along the Fermi surface. Subsequently, we add the nonleading contributions arising from the nonparquet diagrams. As a result of that, we show numerically that the coupling functions either flow to large plateau values or approach zero. Those nonzero plateau values are however sensitive to our discretization procedure. Therefore, we can neither establish their stability nor completely rule out that the plateaus represent some intermediate crossover regime associated with the inexact discretization of the coupled integral equations. At the end, we conclude by discussing how this picture should be altered by the renormalization of the Fermi surface whose effects will be shown in a subsequent work.

II. FERMI SURFACE AND LAGRANGIAN MODEL

Our starting point is a strongly interacting 2D electron gas in the presence of the flat FS shown schematically in Fig.1. In order to keep a closer contact with well-known works in one-dimensional physics[14], we divide the FS into four regions. We restrict the momenta at the FS to the flat parts only. The contributions of the patches perpendicular to the k_x and k_y directions do not mix with each other in our approach. For convenience, we restrict ourselves to the one-electron states labelled by the momenta $p_\perp = k_y$ and $p_\parallel = k_x$ associated with one of the two sets of perpendicular patches. The momenta parallel to the FS are restricted to the interval $-\Delta \leqslant p_\parallel \leqslant \Delta$, where Δ essentially determines the size of the flat patches. The energy dispersion of the single-particle states are given by $\varepsilon_a(\mathbf{p}) = v_F(|p_\perp| - k_F)$ depending only on the momenta perpendicular to the Fermi surface. The label $a = \pm$ refers to the flat sectors at $p_\perp = \pm k_F$ respectively. Here we take $k_F - \lambda \leqslant |p_\perp| \leqslant k_F + \lambda$, where λ is some fixed momentum cut-off. The Fermi momentum k_F is not renormalized in our approach and takes its noninteracting value. We also neglect the Fermi velocity v_F dependence along the FS. This is consistent with the fact that the Fermi surface will not be renormalized in the present work.

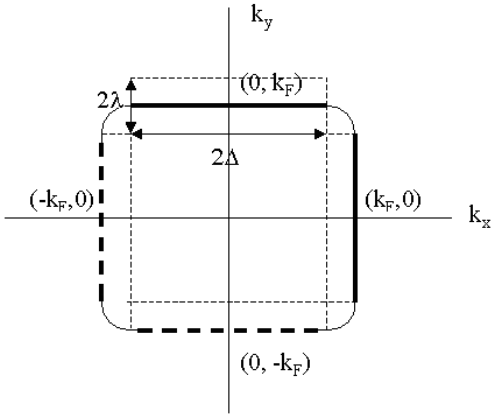

FIG. 1: The 2D flat Fermi surface with rounded corners. We divide it into four regions: two of the solid line type and two of the dashed line type. The perpendicular regions do not mix in our scheme.

The Lagrangian L associated with the 2D flat Fermi surface is given by

$$\begin{aligned} L = & \sum_{\mathbf{p},\sigma,a=\pm} \psi^\dagger_{(a)\sigma}(\mathbf{p}) \left[i\partial_t - v_F(|p_\perp| - k_F) \right] \psi_{(a)\sigma}(\mathbf{p}) \\ & - \frac{1}{V} \sum_{\mathbf{p},\mathbf{q},\mathbf{k}} \sum_{\alpha,\beta,\delta,\gamma} \left[g_2 \delta_{\alpha\delta}\delta_{\beta\gamma} - g_1 \delta_{\alpha\gamma}\delta_{\beta\delta} \right] \\ & \times \psi^\dagger_{(+)\delta}(\mathbf{p}+\mathbf{q}-\mathbf{k}) \psi^\dagger_{(-)\gamma}(\mathbf{k}) \psi_{(-)\beta}(\mathbf{q}) \psi_{(+)\alpha}(\mathbf{p}), \end{aligned} \tag{2.1}$$

where we are following the "g-ology" notation. Here the $\psi^\dagger_{(\pm)}$ and $\psi_{(\pm)}$ are, respectively, the creation and annihilation operators of particles located at the $\pm$ patches. The couplings g_1 and g_2 stand for backscattering and forward scattering. V is the volume of the two-dimensional system which, for convenience, will be set equal to unity

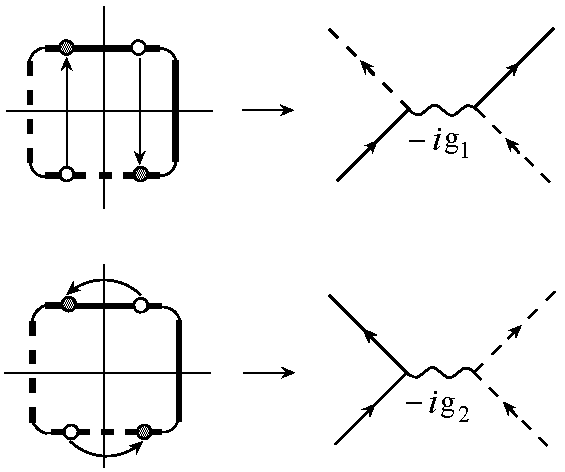

FIG. 2: The interacion processes in the model and the corresponding Feynman rules for the vertices. The g_1 and g_2 couplings stand for backscattering and forward scattering respectively.

from this point on. The graphical representations of the corresponding forward and backscattering interactions are shown schematically in Fig.2. In all Feynman diagrams, the single-particle propagators $G^{(0)}_{(+)}$ and $G^{(0)}_{(-)}$ will be represented by a solid and a dashed line respectively, according to their association with the corresponding FS patches.

In setting up a conventional perturbation theory to do calculations with this model one immediately encounters, in one-loop order, logarithmic divergent particle-particle and particle-hole diagrams[15,16]

$$\Pi^{(0)}\left(q_0, q_\perp = 0, q_\parallel\right) = \int_p G^{(0)}_{(+)}\left(p\right) G^{(0)}_{(-)}\left(-p+q\right), \tag{2.2}$$

$$\chi^{(0)}\left(q_0, q_\perp = -2k_F, q_\parallel\right) = \int_p G^{(0)}_{(+)}\left(p\right) G^{(0)}_{(-)}\left(p+q\right), \tag{2.3}$$

where $p = (p_0, p_\perp, p_\parallel)$ and $\int_p = \int \frac{dp_\parallel}{2\pi}\frac{dp_\perp}{2\pi}\frac{dp_0}{2\pi}$.

Using the single-particle propagators from the non-interacting part of the Lagrangian we find respectively

$$\Pi^{(0)}\left(q_0 = \omega, q_\parallel\right) = i\frac{\left(2\Delta - \left|q_\parallel\right|\right)}{4\pi^2 v_F}\ln\left(\frac{\Omega}{\omega}\right), \tag{2.4}$$

and

$$\chi^{(0)}\left(q_0 = \omega, q_\parallel\right) = -i\frac{\left(2\Delta - \left|q_\parallel\right|\right)}{4\pi^2 v_F}\ln\left(\frac{\Omega}{\omega}\right), \tag{2.5}$$

where $-\Delta \leqslant q_\parallel \leqslant \Delta$, $\Omega = 2v_F\lambda$ is a fixed upper energy cutoff and ω is an energy scale which goes to zero as we approach the Fermi surface. These infrared divergent functions will appear infinitely many times if we attempt to do a perturbative calculation of the interacting one-particle Green's function $G_{(\pm)}(p)$ or the effective two-particle interaction, i.e. the one-particle irreducible function $\Gamma^{(4)}(p_1, p_2, p_3, p_4)$, to infinite order. This will, of course, invalidate any conventional perturbation theory approach to the problem and, at the same time, will make meaningless the direct comparison of our results with experiment. While the experiments find in principle finite values for the measured physical quantities, our perturbative series expansions are plagued with an infinite number of powers of infrared logarithmic singularities.

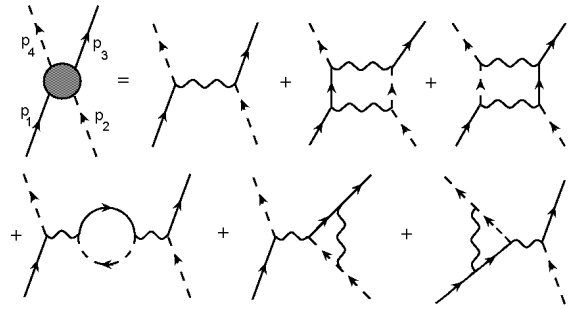

FIG. 3: The Feynman diagrams up to one-loop order for the four-point vertex in the backscattering channel. The single particle propagators are represented by either solid or dashed lines according to their association with the corresponding FS patches.

We circumvent this problem following the field theory procedure of introducing appropriate counterterms in the Lagrangian to render the physical parameters finite in all scattering channels[17]. In doing so, we eliminate the divergences order by order in perturbation theory. What will become clear soon is that the 2D Fermi surface will add important new features in this scheme. The counterterms are now functions of momenta and vary continuously along the FS. In the next section, we begin to show how to implement the fermionic field theory RG in practice by calculating the renormalized one-particle irreducible functions associated with both backscattering and forward scattering up to one-loop order.

III. RENORMALIZED COUPLING FUNCTIONS AT ONE-LOOP ORDER

Let us calculate initially the one-particle irreducible function $\Gamma^{(4)}$ associated with the backscattering channel up to one-loop order. Using appropriate Feynman rules, we arrive at

$$\begin{aligned}\Gamma^{(4)}_1(p_1, p_2, p_3) = &-ig_1 + 2g_1 g_2 \Pi^{(0)}(p_1 + p_2) \\ &-2g_1^2\chi^{(0)}(p_2 - p_3) + 2g_1 g_2 \chi^{(0)}(p_2 - p_3).\end{aligned} \tag{3.1}$$

where it will be implicitly assumed from this point on that $p_4 = p_1 + p_2 - p_3$ by momentum conservation. In addition, we follow the same conventions as before concern-

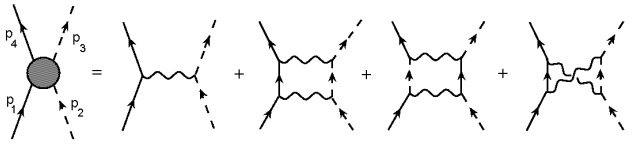

FIG. 4: The Feynman diagrams up to one-loop order for the four-point vertex in the forward scattering channel.

ing integrals and energy-momenta representation. The diagrams corresponding to these contributions are shown schematically in Fig.3.

Let us next perform a similar calculation with the one-particle irreducible function $\Gamma^{(4)}$ associated with the forward scattering channel depicted in Fig.4. Using once again the Feynman rules associated with our initial L, we obtain

$$\Gamma_2^{(4)}\left(p_1,p_2,p_3\right) = -ig_2 + g_1^2\Pi^{(0)}(p_1+p_2) + g_2^2\Pi^{(0)}(p_1+p_2) + g_2^2\chi^{(0)}(p_3-p_1). \tag{3.2}$$

It is clear from those two perturbative series expansions that the internal particle-particle and particle-hole lines will produce logarithmic singularities if the external momenta and energies are located at the Fermi surface. To deal with this problem and to regularize our perturbation expansions, we now invoke the field theory method.

Being the effective two-particle interaction in the backscattering channel, we define the finite one-particle irreducible $\Gamma_1^{(4)}$ such that the renormalized backscattering coupling function $g_{1R}\left(p_{1\parallel},p_{2\parallel},p_{3\parallel};\omega\right)$ is given by

$$\Gamma_1^{(4)}\left(p_1,p_2,p_3\right) = -ig_{1R}\left(p_1,p_2,p_3;\omega\right), \tag{3.3}$$

where $p_{1\perp}=k_F$, $p_{2\perp}=-k_F$, $p_{3\perp}=k_F$, $p_{4\perp}=-k_F$ and the corresponding energy components $p_{10}=p_{20}=\omega/2$, $p_{30}=3\omega/2$ and $p_{40}=-\omega/2$. Similarly for $p_{1\perp}=k_F$, $p_{2\perp}=-k_F$, $p_{3\perp}=-k_F$, $p_{4\perp}=k_F$ and for $p_{10}=p_{20}=\omega/2$, $p_{30}=3\omega/2$ and $p_{40}=-\omega/2$, we relate the finite one-particle irreducible $\Gamma_2^{(4)}$ and the renormalized forward coupling function $g_{2R}\left(p_{1\parallel},p_{2\parallel},p_{3\parallel};\omega\right)$ to each other

$$\Gamma_2^{(4)}\left(p_1,p_2,p_3\right) = -ig_{2R}\left(p_1,p_2,p_3;\omega\right). \tag{3.4}$$

We now go back to our initial Lagrangian model and replace the coupling constants g_1 and g_2 by the renormalized coupling functions $g_{1R}(\{p_{i\parallel}\};\omega)$ and $g_{2R}(\{p_{i\parallel}\};\omega)$ respectively. If we apply the Feynman rules with our new forward and backscattering coupling functions to calculate both $\Gamma_1^{(4)}$ and $\Gamma_2^{(4)}$ at the Fermi surface we find instead

$$\Gamma_1^{(4)} = -ig_{1R}\left(p_{1\parallel},p_{2\parallel},p_{3\parallel}\right) + \frac{i}{4\pi^2 v_F}\Bigg\{\int_{\mathcal{D}_1} dk_\parallel \left[g_{1R}\left(-k_\parallel+p_{1\parallel}+p_{2\parallel},k_\parallel,p_{3\parallel}\right) g_{2R}\left(p_{1\parallel},p_{2\parallel},k_\parallel\right) + g_{2R}\left(k_\parallel,-k_\parallel+p_{1\parallel}+p_{2\parallel},p_{1\parallel}+p_{2\parallel}-p_{3\parallel}\right) g_{1R}\left(p_{1\parallel},p_{2\parallel},k_\parallel\right)\right] + \int_{\mathcal{D}_2} dk_\parallel \left[2g_{1R}\left(p_{1\parallel},p_{2\parallel}-p_{3\parallel}+k_\parallel,k_\parallel\right) \times g_{1R}\left(k_\parallel,p_{2\parallel},p_{3\parallel}\right) - g_{1R}\left(p_{1\parallel},p_{2\parallel}-p_{3\parallel}+k_\parallel,k_\parallel\right) g_{2R}\left(k_\parallel,p_{2\parallel},p_{2\parallel}-p_{3\parallel}+k_\parallel\right) - g_{1R}\left(k_\parallel,p_{2\parallel},p_{3\parallel}\right) \times g_{2R}\left(p_{1\parallel},p_{2\parallel}-p_{3\parallel}+k_\parallel,p_{1\parallel}+p_{2\parallel}-p_{3\parallel}\right)\right]\Bigg\} \ln\left(\frac{\Omega}{\omega}\right), \tag{3.5}$$

and

$$\Gamma_2^{(4)} = -ig_{2R}\left(p_{1\parallel},p_{2\parallel},p_{3\parallel}\right) + \frac{i}{4\pi^2 v_F}\Bigg\{\int_{\mathcal{D}_1} dk_\parallel \left[g_{2R}\left(-k_\parallel+p_{1\parallel}+p_{2\parallel},k_\parallel,p_{3\parallel}\right) g_{2R}\left(p_{1\parallel},p_{2\parallel},k_\parallel\right) + g_{1R}\left(k_\parallel,-k_\parallel+p_{1\parallel}+p_{2\parallel},p_{1\parallel}+p_{2\parallel}-p_{3\parallel}\right) g_{1R}\left(p_{1\parallel},p_{2\parallel},k_\parallel\right)\right] - \int_{\mathcal{D}_3} dk_\parallel \left[g_{2R}\left(p_{1\parallel},p_{3\parallel}-p_{1\parallel}+k_\parallel,p_{3\parallel}\right) \times g_{2R}\left(k_\parallel,p_{2\parallel},p_{3\parallel}-p_{1\parallel}+k_\parallel\right)\right]\Bigg\} \ln\left(\frac{\Omega}{\omega}\right), \tag{3.6}$$

where all the domains of integration $\mathcal{D}_i$ are given explicitly in Appendix A. As it stands, the $\Gamma_i^{(4)}$'s are divergent as $\omega\to 0$, contradicting our earlier assumptions given in Eqs.(3.3) and (3.4). To remedy the situation, we add a new term to L

$$-\sum_{\mathbf{p},\mathbf{q},\mathbf{k}}\sum_{\alpha,\beta,\delta,\gamma}\left[\Delta g_2\delta_{\alpha\delta}\delta_{\beta\gamma}-\Delta g_1\delta_{\alpha\gamma}\delta_{\beta\delta}\right]\psi^\dagger_{(+)\delta}\left(\mathbf{p}+\mathbf{q}-\mathbf{k}\right)\psi^\dagger_{(-)\gamma}\left(\mathbf{k}\right)\psi_{(-)\beta}\left(\mathbf{q}\right)\psi_{(+)\alpha}\left(\mathbf{p}\right), \tag{3.7}$$

where

$$\Delta g_{1R}\left(p_{1\|},p_{2\|},p_{3\|};\omega\right)=\frac{1}{4\pi^2 v_F}\Big\{\int_{\mathcal{D}_1}dk_\|\left[g_{1R}\left(-k_\|+p_{1\|}+p_{2\|},k_\|,p_{3\|}\right)g_{2R}\left(p_{1\|},p_{2\|},k_\|\right)+g_{1R}\left(p_{1\|},p_{2\|},k_\|\right)\right.$$
$$\left.\times\, g_{2R}\left(k_\|,-k_\|+p_{1\|}+p_{2\|},p_{1\|}+p_{2\|}-p_{3\|}\right)\right]+\int_{\mathcal{D}_2}dk_\|\left[2g_{1R}\left(p_{1\|},p_{2\|}-p_{3\|}+k_\|,k_\|\right)g_{1R}\left(k_\|,p_{2\|},p_{3\|}\right)\right.$$
$$-g_{1R}\left(p_{1\|},p_{2\|}-p_{3\|}+k_\|,k_\|\right)g_{2R}\left(k_\|,p_{2\|},p_{2\|}-p_{3\|}+k_\|\right)-g_{2R}\left(p_{1\|},p_{2\|}-p_{3\|}+k_\|,p_{1\|}+p_{2\|}-p_{3\|}\right)$$
$$\left.\left.\times\, g_{1R}\left(k_\|,p_{2\|},p_{3\|}\right)\right]\Big\}\ln\left(\frac{\Omega}{\omega}\right), \tag{3.8}$$

and

$$\Delta g_{2R}\left(p_{1\|},p_{2\|},p_{3\|};\omega\right)=\frac{1}{4\pi^2 v_F}\Big\{\int_{\mathcal{D}_1}dk_\|\left[g_{2R}\left(-k_\|+p_{1\|}+p_{2\|},k_\|,p_{3\|}\right)g_{2R}\left(p_{1\|},p_{2\|},k_\|\right)+g_{1R}\left(p_{1\|},p_{2\|},k_\|\right)\right.$$
$$\left.\times\, g_{1R}\left(k_\|,-k_\|+p_{1\|}+p_{2\|},p_{1\|}+p_{2\|}-p_{3\|}\right)\right]-\int_{\mathcal{D}_3}dk_\|\left[g_{2R}\left(p_{1\|},p_{3\|}-p_{1\|}+k_\|,p_{3\|}\right)\right.$$
$$\left.\left.\times\, g_{2R}\left(k_\|,p_{2\|},p_{3\|}-p_{1\|}+k_\|\right)\right]\Big\}\ln\left(\frac{\Omega}{\omega}\right). \tag{3.9}$$

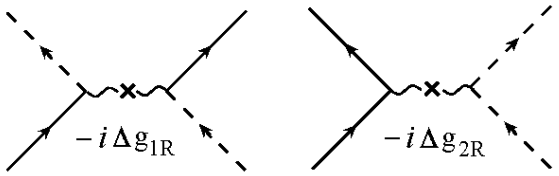

FIG. 5: The additional Feynman rules for the counterterm vertices.

The Δg_i's are continuous functions of the scale ω and of the components of external momenta $p_{1\|}$, $p_{2\|}$, $p_{3\|}$ only, since their related $p_{i\perp}$ components are fixed at the Fermi surface. The presence of these new terms in the Lagrangian results in additional Feynman rules represented in Fig.5.

We can adjust the counterterms such that all divergences are exactly cancelled in our series expansion for $\Gamma_1^{(4)}$ and $\Gamma_2^{(4)}$ in one-loop order. But the price we pay for this is the appearance of an energy scale ω. All physical quantities now depend on this new scale parameter. However, the original theory does not know anything about ω, i.e., the initial parameters do not depend on the scale. This naturally leads us to the renormalization group conditions for the renormalized coupling functions

$$\omega\frac{d}{d\omega}\left(g_{1R}+\Delta g_{1R}\right)=0, \tag{3.10}$$

and

$$\omega\frac{d}{d\omega}\left(g_{2R}+\Delta g_{2R}\right)=0. \tag{3.11}$$

The RG flow equations for the renormalized coupling functions follow immediately from this. We therefore find in one-loop order

$$\omega\frac{dg_{1R}(p_{1\|},p_{2\|},p_{3\|})}{d\omega}=\frac{1}{4\pi^2 v_F}\Big\{\int_{\mathcal{D}_1}dk_\|\left[g_{1R}\left(-k_\|+p_{1\|}+p_{2\|},k_\|,p_{3\|}\right)g_{2R}\left(p_{1\|},p_{2\|},k_\|\right)\right.$$
$$\left.+\, g_{2R}\left(k_\|,-k_\|+p_{1\|}+p_{2\|},p_{1\|}+p_{2\|}-p_{3\|}\right)g_{1R}\left(p_{1\|},p_{2\|},k_\|\right)\right]$$
$$+\int_{\mathcal{D}_2}dk_\|\left[2g_{1R}\left(p_{1\|},p_{2\|}-p_{3\|}+k_\|,k_\|\right)g_{1R}\left(k_\|,p_{2\|},p_{3\|}\right)\right.$$
$$-g_{1R}\left(p_{1\|},p_{2\|}-p_{3\|}+k_\|,k_\|\right)g_{2R}\left(k_\|,p_{2\|},p_{2\|}-p_{3\|}+k_\|\right)$$
$$\left.\left.-\, g_{2R}\left(p_{1\|},p_{2\|}-p_{3\|}+k_\|,p_{1\|}+p_{2\|}-p_{3\|}\right)g_{1R}\left(k_\|,p_{2\|},p_{3\|}\right)\right]\Big\}, \tag{3.12}$$

and

$$\omega\frac{dg_{2R}(p_{1\parallel},p_{2\parallel},p_{3\parallel})}{d\omega}=\frac{1}{4\pi^2v_F}\Big\{\int_{\mathcal{D}_1}dk_\parallel\left[g_{2R}\left(-k_\parallel+p_{1\parallel}+p_{2\parallel},k_\parallel,p_{3\parallel}\right)g_{2R}\left(p_{1\parallel},p_{2\parallel},k_\parallel\right)\right.$$
$$\left.+\,g_{1R}\left(k_\parallel,-k_\parallel+p_{1\parallel}+p_{2\parallel},p_{1\parallel}+p_{2\parallel}-p_{3\parallel}\right)g_{1R}\left(p_{1\parallel},p_{2\parallel},k_\parallel\right)\right]$$
$$-\int_{\mathcal{D}_3}dk_\parallel\left[g_{2R}\left(p_{1\parallel},p_{3\parallel}-p_{1\parallel}+k_\parallel,p_{3\parallel}\right)g_{2R}\left(k_\parallel,p_{2\parallel},p_{3\parallel}-p_{1\parallel}+k_\parallel\right)\right]\Big\}. \tag{3.13}$$

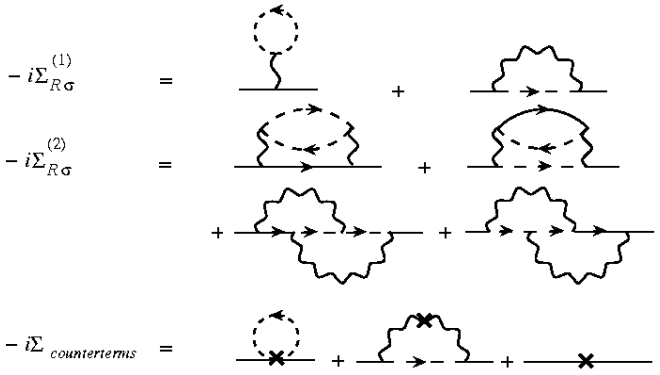

FIG. 6: The diagrams for the self-energy calculation up to two-loop order. The last diagram of $-i\Sigma_{counterterms}$ is not computed at this stage. It represents the ΔZ contribution which will be added later on.

These RG equations are exactly equal to the ones obtained by Zheleznyak *et al.*[6] using the parquet method. In fact, performing one-loop RG calculations is equivalent to sum the parquet class of diagrams up to infinite order.

Having shown in detail how the RG field theory operates in one-loop order we can now proceed to calculate with this method the electron self-energy up to two loops.

IV. SELF-ENERGY AND QUASIPARTICLE WEIGHT UP TO TWO LOOPS

The field theory RG eliminates the infrared divergences order by order in the coupling functions. We do this by invoking the usual Feynman rules at each order to obtain finite result in terms of the renormalized physical quantities. Let us continue with the use of this method to obtain the electron self-energy up to second order. Using our already modified Feynman rules we have

$$\Sigma_{R\sigma}\left(p\right)=\Sigma^{(1)}_{R\sigma}+\Sigma^{(2)}_{R\sigma}+\Sigma_{counterterms}. \tag{4.1}$$

We show the diagrams corresponding to each of those contributions in Fig.6. The one-loop contributions $-i\Sigma^{(1)}_{R\sigma}$ and the first two diagrams of $-i\Sigma_{counterterms}$ produce a shift in k_F and they are crucial for the renormalization of the Fermi velocity and of the Fermi surface itself[18]. Those aspects will be discussed in a subsequent paper. We neglect their contributions in the present work altogether. Let us therefore concentrate our attention in the two-loop terms $-i\Sigma^{(2)}_{R\sigma}$. We find

$$-i\Sigma^{(2)}_{R\sigma}\left(p_0,p_\perp,p_\parallel;\omega\right)=\frac{i}{64\pi^4v_F^2}\left(p_0-v_F\left(p_\perp-k_F\right)\right)\int_{\mathcal{D}_4}dk_\parallel dq_\parallel[2g_{1R}\left(-k_\parallel+p_\parallel+q_\parallel,k_\parallel,q_\parallel\right)$$
$$\times\,g_{1R}\left(p_\parallel,q_\parallel,k_\parallel\right)+2g_{2R}\left(p_\parallel,q_\parallel,-k_\parallel+p_\parallel+q_\parallel\right)g_{2R}\left(k_\parallel,-k_\parallel+p_\parallel+q_\parallel,q_\parallel\right)-g_{1R}\left(p_\parallel,q_\parallel,k_\parallel\right)$$
$$\times\,g_{2R}\left(k_\parallel,-k_\parallel+p_\parallel+q_\parallel,q_\parallel\right)-g_{2R}\left(p_\parallel,q_\parallel,-k_\parallel+p_\parallel+q_\parallel\right)g_{1R}\left(k_\parallel,-k_\parallel+p_\parallel+q_\parallel,p_\parallel\right)]$$
$$\times\left[\ln\left(\frac{\Omega-v_F\left(p_\perp-k_F\right)-p_0-i\delta}{v_F\left(p_\perp-k_F\right)-p_0-i\delta}\right)+\ln\left(\frac{\Omega-v_F\left(p_\perp-k_F\right)+p_0-i\delta}{v_F\left(p_\perp-k_F\right)+p_0-i\delta}\right)\right]. \tag{4.2}$$

where $\mathcal{D}_4$ is given in Appendix A. If we take the limits $\omega\to 0$ with $p_\perp=k_F$ or $v_F\left(p_\perp-k_F\right)=\omega\to 0$ at $p_0=0$ our perturbation theory produces an undesirable nonanalyticity at the FS. The way to eliminate this is again to add a new term to our Lagrangian of the form

$$F\left(p_\parallel;\omega\right)\sum_{\mathbf{p},\sigma,a=\pm}\psi^\dagger_{(a)\sigma}\left(\mathbf{p}\right)\left[i\partial_t-v_F\left(p_\perp-k_F\right)\right]\psi_{(a)\sigma}\left(\mathbf{p}\right). \tag{4.3}$$

With this, the new "noninteracting" Lagrangian now

reads

$$\sum_{\mathbf{p},\sigma,a=\pm}\left(1+F\left(p_{\parallel};\omega\right)\right)$$
$$\times\psi^{\dagger}_{(a)\sigma}\left(\mathbf{p}\right)\left[i\partial_t-v_F\left(p_{\perp}-k_F\right)\right]\psi_{(a)\sigma}\left(\mathbf{p}\right). \tag{4.4}$$

Let us define $F\left(p_{\parallel};\omega\right)=\Delta Z\left(p_{\parallel};\omega\right)=Z\left(p_{\parallel};\omega\right)-1$. Now, in passing, we notice that the main effect of this new counterterm is to renormalize the fermion field

$$\psi_{(a)\sigma}\left(\mathbf{p}\right)\rightarrow Z^{\frac{1}{2}}\left(p_{\parallel};\omega\right)\psi_{(a)\sigma}\left(\mathbf{p}\right). \tag{4.5}$$

To determine the function $\Delta Z\left(p_{\parallel};\omega\right)$ we consider the inverse of the renormalized one-particle Green's function $\Gamma^{(2)}_{R\sigma}\left(p\right)$. Let us define $\Gamma^{(2)}_{R\sigma}$ such that at $p_{\perp}=k_F$ and $p_0=\omega$

$$\Gamma^{(2)}_{R\sigma}\left(p_0=\omega,p_{\perp}=k_F,p_{\parallel}\right)=\omega. \tag{4.6}$$

Taking into account that

$$\Gamma^{(2)}_{R\sigma}\left(p\right)=Z\left(p_{\parallel};\omega\right)\left[p_0-v_F\left(p_{\perp}-k_F\right)\right]-\Sigma^{(2)}_{R\sigma}\left(p_0,p_{\perp},p_{\parallel};\omega\right), \tag{4.7}$$

it follows from our previous result that

$$Z\left(p_{\parallel};\omega\right)=1-\frac{1}{32\pi^4v_F^2}\int_{\mathcal{D}_4}dk_{\parallel}dq_{\parallel}[2g_{1R}\left(-k_{\parallel}+p_{\parallel}+q_{\parallel},k_{\parallel},q_{\parallel}\right)g_{1R}\left(p_{\parallel},q_{\parallel},k_{\parallel}\right)+2g_{2R}\left(p_{\parallel},q_{\parallel},-k_{\parallel}+p_{\parallel}+q_{\parallel}\right)$$
$$\times g_{2R}\left(k_{\parallel},-k_{\parallel}+p_{\parallel}+q_{\parallel},q_{\parallel}\right)-g_{1R}\left(p_{\parallel},q_{\parallel},k_{\parallel}\right)g_{2R}\left(k_{\parallel},-k_{\parallel}+p_{\parallel}+q_{\parallel},q_{\parallel}\right)-g_{2R}\left(p_{\parallel},q_{\parallel},-k_{\parallel}+p_{\parallel}+q_{\parallel}\right)$$
$$\times g_{1R}\left(k_{\parallel},-k_{\parallel}+p_{\parallel}+q_{\parallel},p_{\parallel}\right)]\ln\left(\frac{\Omega}{\omega}\right). \tag{4.8}$$

This reproduces the result obtained earlier by Kishine and Yonemitsu[19] within a Wilsonian RG framework. In addition to that, making use of Eq.(4.8) we obtain the following RG equation for the quasiparticle weight

$$\omega\frac{\partial Z\left(p_{\parallel};\omega\right)}{\partial\omega}=\gamma Z\left(p_{\parallel};\omega\right), \tag{4.9}$$

where the anomalous dimension γ is given by

$$\gamma\left(p_{\parallel}\right)=\frac{1}{32\pi^4v_F^2}\int_{\mathcal{D}_4}dk_{\parallel}dq_{\parallel}[2g_{1R}\left(-k_{\parallel}+p_{\parallel}+q_{\parallel},k_{\parallel},q_{\parallel}\right)g_{1R}\left(p_{\parallel},q_{\parallel},k_{\parallel}\right)+2g_{2R}\left(p_{\parallel},q_{\parallel},-k_{\parallel}+p_{\parallel}+q_{\parallel}\right)$$
$$\times g_{2R}\left(k_{\parallel},-k_{\parallel}+p_{\parallel}+q_{\parallel},q_{\parallel}\right)-g_{1R}\left(p_{\parallel},q_{\parallel},k_{\parallel}\right)g_{2R}\left(k_{\parallel},-k_{\parallel}+p_{\parallel}+q_{\parallel},q_{\parallel}\right)-g_{2R}\left(p_{\parallel},q_{\parallel},-k_{\parallel}+p_{\parallel}+q_{\parallel}\right)$$
$$\times g_{1R}\left(k_{\parallel},-k_{\parallel}+p_{\parallel}+q_{\parallel},p_{\parallel}\right)]. \tag{4.10}$$

Before proceeding with the full calculation of the RG equations for the renormalized coupling functions in two-loop order we call attention to the fact that up to now, due to the addition of several counterterms, our original Lagrangian can be written as

$$L=\sum_{\mathbf{p},\sigma,a=\pm}Z\psi^{\dagger}_{(a)\sigma}\left(\mathbf{p}\right)\left[i\partial_t-v_F\left(p_{\perp}-k_F\right)\right]\psi_{(a)\sigma}\left(\mathbf{p}\right)$$
$$-\sum_{\mathbf{p},\mathbf{q},\mathbf{k}}\sum_{\alpha,\beta,\delta,\gamma}\left[\prod_{i=1}^{4}Z\left(p_{i\parallel}\right)\right]^{\frac{1}{2}}\left[g_{2B}\delta_{\alpha\delta}\delta_{\beta\gamma}-g_{1B}\delta_{\alpha\gamma}\delta_{\beta\delta}\right]$$
$$\times\psi^{\dagger}_{(+)\delta}\left(\mathbf{p}+\mathbf{q}-\mathbf{k}\right)\psi^{\dagger}_{(-)\gamma}\left(\mathbf{k}\right)\psi_{(-)\beta}\left(\mathbf{q}\right)\psi_{(+)\alpha}\left(\mathbf{p}\right), \tag{4.11}$$

where g_{1B} and g_{2B} are the bare couplings which are in turn defined to be

$$g_{iB}=\left[\prod_{i=1}^{4}Z\left(p_{i\parallel}\right)\right]^{-\frac{1}{2}}\left(g_{iR}+\Delta g_{iR}\right). \tag{4.12}$$

Together with the quasiparticle weight, they will render the theory finite to all orders in perturbation theory as will become clear soon.

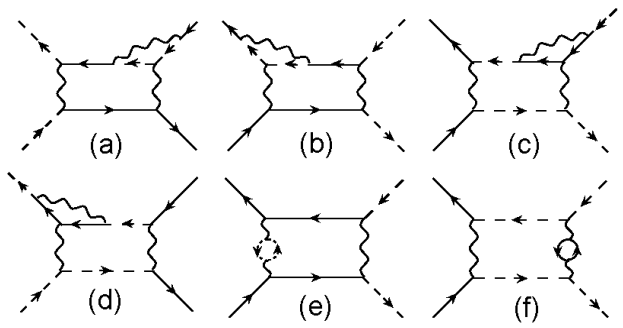

FIG. 7: The nonparquet diagrams for the renormalized four-point vertex in the backscattering channel.

V. RG EQUATIONS AT TWO-LOOP ORDER

For convenience, let us rewrite our renormalized Lagrangian in the form

$$\begin{aligned} L = & \sum_{\mathbf{p},\sigma,a=\pm} \psi^{\dagger}_{(a)\sigma}\left(\mathbf{p}\right)\left[i\partial_t - v_F\left(p_\perp - k_F\right)\right]\psi_{(a)\sigma}\left(\mathbf{p}\right) \\ & - \sum_{\mathbf{p},\mathbf{q},\mathbf{k}}\sum_{\alpha,\beta,\delta,\gamma}\left[g_{2R}\delta_{\alpha\delta}\delta_{\beta\gamma} - g_{1R}\delta_{\alpha\gamma}\delta_{\beta\delta}\right] \\ & \times \psi^{\dagger}_{(+)\delta}\left(\mathbf{p}+\mathbf{q}-\mathbf{k}\right)\psi^{\dagger}_{(-)\gamma}\left(\mathbf{k}\right)\psi_{(-)\beta}\left(\mathbf{q}\right)\psi_{(+)\alpha}\left(\mathbf{p}\right) \\ & + \sum_{\mathbf{p},\sigma,a=\pm} \Delta Z\psi^{\dagger}_{(a)\sigma}\left(\mathbf{p}\right)\left[i\partial_t - v_F\left(p_\perp - k_F\right)\right]\psi_{(a)\sigma}\left(\mathbf{p}\right) \\ & - \sum_{\mathbf{p},\mathbf{q},\mathbf{k}}\sum_{\alpha,\beta,\delta,\gamma}\left[\Delta g_{2R}\delta_{\alpha\delta}\delta_{\beta\gamma} - \Delta g_{1R}\delta_{\alpha\gamma}\delta_{\beta\delta}\right] \\ & \times \psi^{\dagger}_{(+)\delta}\left(\mathbf{p}+\mathbf{q}-\mathbf{k}\right)\psi^{\dagger}_{(-)\gamma}\left(\mathbf{k}\right)\psi_{(-)\beta}\left(\mathbf{q}\right)\psi_{(+)\alpha}\left(\mathbf{p}\right). \end{aligned} \tag{5.1}$$

Let us initially consider the diagrams obtained with our new Feynman rules generated by this Lagrangian in two-loop order. At this point, we only mention that to avoid double-counting of diagrams we split up the counterterms into separate blocks. There are several equivalence relations between diagrams generated by the different constituent blocks. This will be explained further in Appendix B. Taking all this into consideration, the contributions due to the counterterms Δg_{1R} and Δg_{2R} cancel exactly all the diagrams which are of the order of $\ln^2\left(\Omega/\omega\right)$ in the vicinity of the Fermi surface. As a result, in third-order, the only remaining $\ln\left(\Omega/\omega\right)$ divergent contributions are produced by the so-called nonparquet diagrams.

We display the nonparquet diagrams for g_{1R} in Fig.7. In view of that, to be consistent with the RG condition given in Eq.(3.3), we have therefore to redefine Δg_{1R} using the same values for energies and momentum components perpendicular to FS as before. We now find

$$\begin{aligned} \Delta g_{1R}\left(p_{1\parallel},p_{2\parallel},p_{3\parallel}\right) = & \Delta g^{1-loop}_{1R} + \Delta g^{2-loop}_{1R(a)} + \Delta g^{2-loop}_{1R(b)} \\ & + \Delta g^{2-loop}_{1R(c)} + \Delta g^{2-loop}_{1R(d)} + \Delta g^{2-loop}_{1R(e)} + \Delta g^{2-loop}_{1R(f)}, \end{aligned} \tag{5.2}$$

where the $\Delta g^{2-loop}_{1R(x)}$, with $x = a...f$, are given explicitly in Appendix A.

We can follow the same procedure to determine Δg_{2R} in two-loop order. The nonparquet diagrams for g_{2R} are displayed in Fig.8. As before, we now get

$$\begin{aligned} \Delta g_{2R}\left(p_{1\parallel},p_{2\parallel},p_{3\parallel}\right) = & \Delta g^{1-loop}_{2R} + \Delta g^{2-loop}_{2R(a)} + \Delta g^{2-loop}_{2R(b)} \\ & + \Delta g^{2-loop}_{2R(c)} + \Delta g^{2-loop}_{2R(d)} + \Delta g^{2-loop}_{2R(e)} + \Delta g^{2-loop}_{2R(f)} \\ & + \Delta g^{2-loop}_{2R(g)} + \Delta g^{2-loop}_{2R(h)} + \Delta g^{2-loop}_{2R(i)} + \Delta g^{2-loop}_{2R(j)}, \end{aligned} \tag{5.3}$$

where the $\Delta g^{2-loop}_{2R(x)}$, with $x = a...j$, are given explicitly in Appendix A.

With the expressions of both Δg_{1R} and Δg_{2R} up to two-loop order we can proceed with the calculation of the accompanying RG equations for the g_{iR}'s. Taking into account the associated Z factors for the external momenta and the RG conditions for the bare coupling functions $dg_{iB}/d\omega = 0$ together with Eq.(4.10) we obtain immediately the two-loop RG equations

$$\begin{aligned} \omega\frac{dg_{iR}\left(p_{1\parallel},p_{2\parallel},p_{3\parallel}\right)}{d\omega} = & \quad \frac{1}{2}\sum_{j=1}^{4}\gamma\left(p_{j\parallel}\right)g_{iR}\left(p_{1\parallel},p_{2\parallel},p_{3\parallel}\right) \\ & -\omega\frac{\partial\Delta g_{iR}\left(p_{1\parallel},p_{2\parallel},p_{3\parallel}\right)}{\partial\omega}. \end{aligned} \tag{5.4}$$

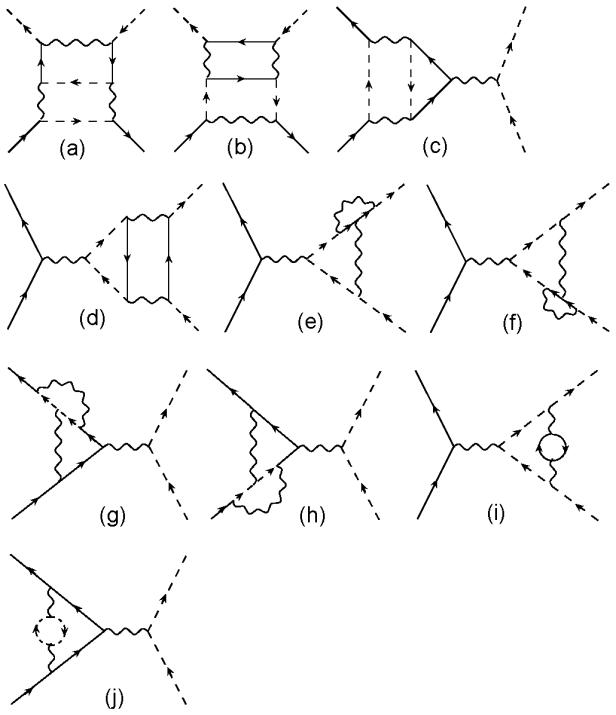

FIG. 8: The nonparquet diagrams for the renormalized four-point vertex in the forward scattering channel.

VI. NUMERICAL RESULTS

Since it is impossible to solve all these RG equations analytically, we have to resort to numerical methods in order to estimate how the coupling functions change as we vary the scale ω to take the physical system towards the FS. Here the basic idea is to discretize the FS continuum replacing the interval $-\Delta \leqslant p_{\parallel} \leqslant \Delta$ by a discrete set of 33 points. For convenience, we use $\omega = \Omega \exp(-l)$, where $\Omega = 2k_F\lambda$ with l being our RG step. We will choose $\Omega/\Delta = 1$. In view of our choice of points for the FS, we are only allowed to go up to $l \approx 2.8$ in the RG flow to avoid the distance ω to the FS being smaller than the distance between points since the discretization procedure no longer applies in this case.

The choice of the initial conditions at $l = 0$ in the RG equations are, in principle, arbitrary. This is related to the fact that one may choose any microscopic model to start with in order to study its low-energy properties. Since we are most interested in relating our results to a repulsive Hubbard model in 2D we initially set the couplings equal to a Hubbard on-site repulsive interaction parameter U in our numerical scheme. As we will see shortly, the RG flows are very sensitive to this initial value. The physical nature of the resulting state is influenced directly by that choice.

In order to show this, at a first stage, we choose $\overline{g}_{1R} = \overline{g}_{2R} = 10$, where $\overline{g}_{iR} = g_{iR}/\pi v_F$. Here, we apply the standard fourth-order Runge-Kutta method to calculate the flow of the couplings $\overline{g}_{1R}$ and $\overline{g}_{2R}$ self-consistently. We will present our results for three cases. The first one is the one-loop approach. Next, we move on to a somewhat intermediate step which includes the contributions of the self-energy or the Z factor feedback into the one-loop RG equations and analyze the corresponding flows. Then we present the full two-loop order RG approach, which includes, in addition to the self-energy feedback, the so-called nonparquet diagram contributions in the RG equations. We will show that in this final case the RG flows are very different from the one-loop case in view of the fact that the quasiparticle weight Z becomes very strongly suppressed as we approach the FS.

Later on, we will change the initial condition, choosing a lower value for the renormalized couplings in order to contrast it with the previous choice. We take $\overline{g}_{1R} = \overline{g}_{2R} = 1$. We will see in this case that since the quasiparticle weight does not change much from its unity initial value, the feedback effect of that factor into the RG equations is not very drastic. As a result, the two-loop flows will resemble very much the corresponding one-loop flow for this particular choice of initial interaction strength.

A. One-loop RG approach

The one-loop results are depicted in Figs.9 and 10. In them, we observe that even though the couplings are initially constant (in our case, equal to ten), they acquire a distinct momentum dependence as we approach the FS. In addition, there are no fixed points in the flow, and all coupling values go unequivocally to a strong coupling regime.

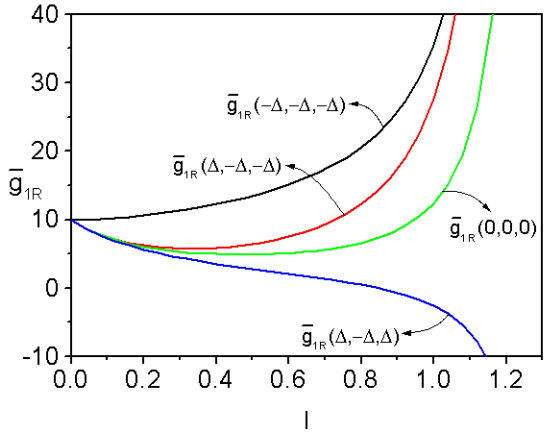

FIG. 9: The one-loop RG flow of $\overline{g}_{1R}(p_{1\parallel}, p_{2\parallel}, p_{3\parallel})$ for some choices of momenta .

This result is consistent with other approaches based on a one-loop order perturbative expansion such as the so-called parquet method and other RG schemes, which predict an instability towards an insulating spin density wave state with no sign of nonconventional metallic behavior ever to be found in the physical system[6].

However, in all those approaches, the quasiparticle weight Z is always equal to unity throughout the calculation. This should be contrasted with the situation in which, due to interactions, the quasiparticle weight might approach zero as well. To discuss what happens in this case, we move on to the next step, which is the inclusion

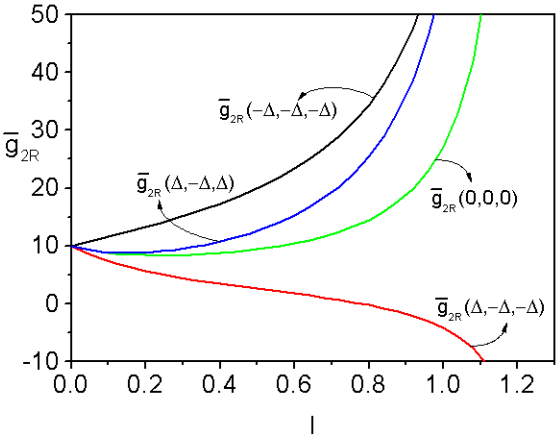

FIG. 10: The one-loop RG flow of $\overline{g}_{2R}(p_{1\parallel}, p_{2\parallel}, p_{3\parallel})$ for some choices of momenta .

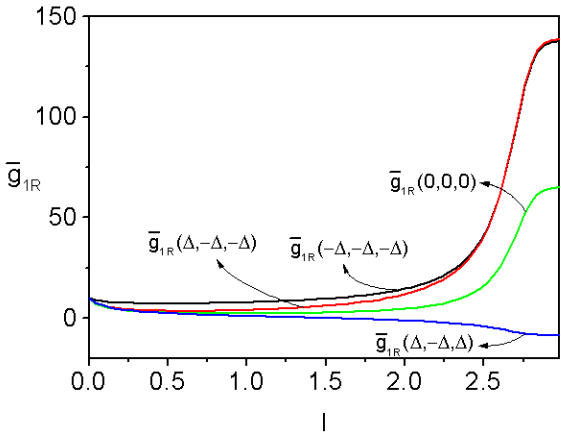

FIG. 11: The one-loop with the Z factor RG flow of $\overline{g}_{1R}(p_{1\|}, p_{2\|}, p_{3\|})$ for some choices of momenta.

of the Z factor feedback into the RG flow equations.

B. One-loop with the Z factor approach

For this case, we depict the results in Figs.11 and 12. In that intermediate approach, which was also discussed by Kishine and Yonemitsu[19], we observe that the initial tendency from one-loop analysis for the couplings to go to a strong coupling regime is preserved. However, as the suppression of Z becomes prominent the flows seem to stop at fixed values. In view of the fact that those values are sensitive to our discretization procedure, we can not associate those results with the existence of stable fixed points. If one increases the number of points necessary for discretizing the FS by some factor, the fixed values (or the plateaus in the figures) increase approximately by the same factor. They should reach a higher bound regardless of the number of points in the discretization procedure in order to be characterized as true fixed points of our RG approach.

Since this last approach is not yet a complete two-loop calculation anyway, we move on to the calculation of the full two-loop RG equations for our problem.

C. The full two-loop approach

In this final case, we solve Eq.(5.4) numerically including both the self-energy feedback and the nonparquet diagram contributions for two different choices of initial conditions $\overline{g}_{1R} = \overline{g}_{2R} = 10$, and $\overline{g}_{1R} = \overline{g}_{2R} = 1$.

For the first choice, the results are shown in Figs.13 and 14. In these figures, we observe that the RG flows, at least qualitatively, do not change much from the previous case. Again, we verify the initial one-loop tendency to flow to a strong coupling regime, but as soon as the Z effect becomes important the rate of change of the couplings reduces abruptly. However, the renormalized coupling functions do not saturate as in the previous case (the above-mentioned plateaus). Although the couplings seem to reach a plateau regime they now in fact change their values continuously at a very slow rate.

Since these two-loop results are directly associated with the effects produced by the quasiparticle weight we might as well analyze the flow as we approach the FS. In order to do that, we must also calculate Eq.(4.9) self-consistently using the same method described above. This equation is solved numerically assuming that for $l = 0$ the quasiparticle weight $Z(l = 0) = 1$. In doing that, we observe numerically a rapid and very anisotropic suppression of Z for a moderate coupling regime when we approach the FS (see Fig.15). The quasiparticle weight

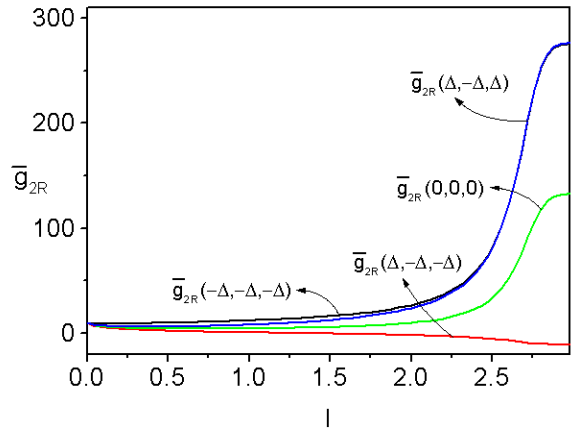

FIG. 12: The one-loop with the Z factor RG flow of $\overline{g}_{2R}(p_{1\|}, p_{2\|}, p_{3\|})$ for some choices of momenta.

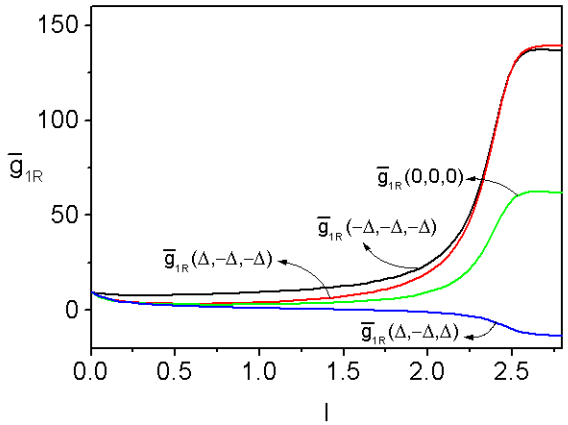

FIG. 13: The full two-loop RG flow of $\overline{g}_{1R}(p_{1\|}, p_{2\|}, p_{3\|})$ for some choices of momenta.

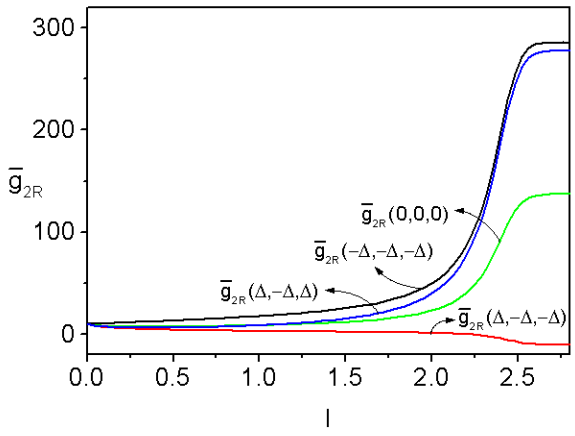

FIG. 14: The full two-loop RG flow of $\overline{g}_{2R}(p_{1\|}, p_{2\|}, p_{3\|})$ for some choices of momenta.

vanishes faster at the center parts of the square FS, i.e. in the $(\pi, 0)$ or $(0, \pi)$-directions. This is in qualitative agreement with Kishine and Yonemitsu[19], although they ignore the nonparquet contributions and hence they do not perform a full two-loop calculation.

Besides the rapid suppression of the quasiparticle weight Z, the two-loop flow of the coupling functions displays other crucial differences in contrast with the one-loop case. While in the one-loop order all couplings seem to increase indefinitely, this is certainly not the case in two-loop. There exists also many couplings which go to zero continuously as we approach the FS. In fact, whenever $\overline{g}_i\left(p_{1\|}, p_{2\|}, p_{3\|}\right)$ is such that $p_{1\|} \neq p_{2\|} \neq p_{3\|}$, the couplings renormalize to zero and are irrelevant in the RG sense. In Fig.16, we show some couplings which belong to this class.

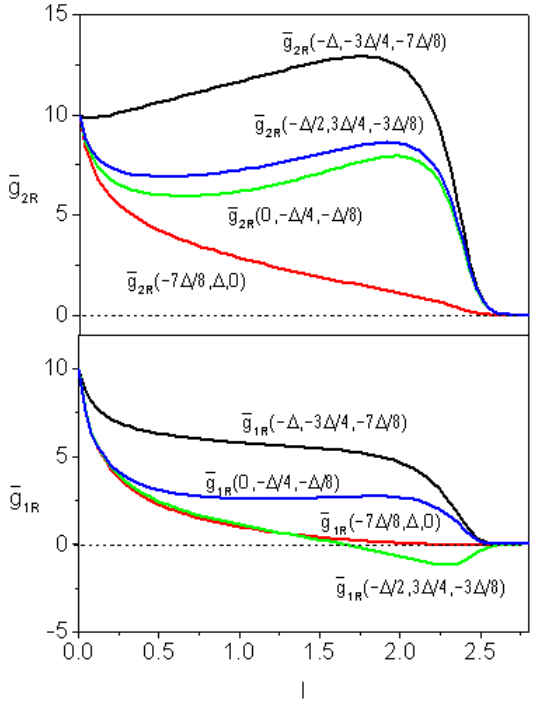

FIG. 16: The vanishing of $\overline{g}_{2R}(p_{1\|}, p_{2\|}, p_{3\|})$ and $\overline{g}_{1R}(p_{1\|}, p_{2\|}, p_{3\|})$ for some choices of momenta.

Now, let us move on to the second choice of initial condition for the couplings, i.e. $\overline{g}_{1R} = \overline{g}_{2R} = 1$. Since we already know that the distinct two-loop features are directly related to what happens to the quasiparticle weight, we will limit our RG analysis to the investigation of the Z flow in this case. As we see from Fig.17, Z is only mildly different from unity in the RG flow. As

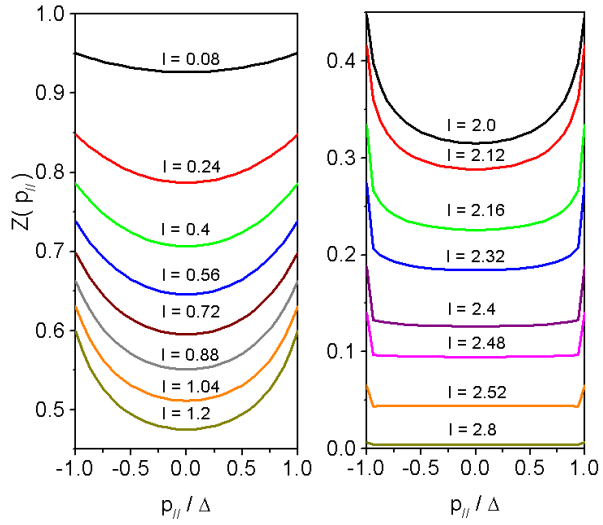

FIG. 15: The RG flow for the quasiparticle weight as a function of the momentum $p_{\|}$ along the FS for $\overline{g}_{1R}(l = 0) = \overline{g}_{2R}(l = 0) = 10$.

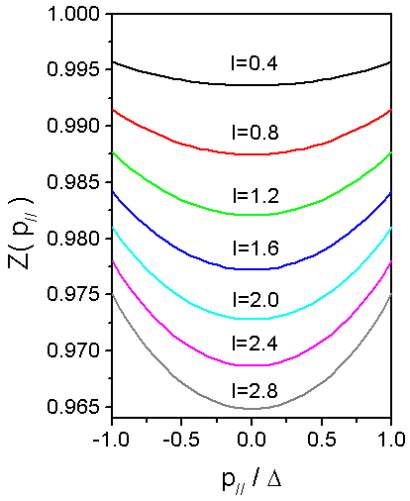

FIG. 17: The RG flow for the quasiparticle weight as a function of the momentum $p_{\|}$ along the FS for $\overline{g}_{1R}(l = 0) = \overline{g}_{2R}(l = 0) = 1$.

a result, the corresponding two-loop flows are very similar to the one-loop flow in this case. In order words, as expected, for initial weak coupling strengths only, it is a reasonable approximation to keep $Z = 1$ fixed throughout the calculation.

Therefore, we observe that models with different physical initial coupling strengths may produce ultimately very different physical states. In our numerical estimates, there is a clear indication of crossover behavior between the regimes defined either by a strongly suppressed quasiparticle weight or a Z nearly equal to unity when we vary the initial values of the couplings.

VII. CONCLUSION

In summary, we showed in full detail a two-loop field theoretical RG calculation for a square and fixed two-dimensional FS with rounded corners. We neglected Umklapp effects at this stage since they only occur when the distance between the parallel FS patches is equal to π. We derived explicitly the Feynman rules of the renormalized Lagrangian which regularize all the divergences generated by perturbation theory. We did that by constructing appropriate counterterms order by order in perturbation theory. Contrary to what happens in local field theory models, those counterterms are now functions of momenta varying continuously along the Fermi surface. We showed that our method reproduces the results of other RG schemes in one-loop order with all the coupling functions flowing unequivocally to strong coupling. This behavior is typical of the dominant spin-density wave instability in that regime, which signals antiferromagnetic ordering as well as the Mott insulating condition.

Then, we moved on to the calculation of the self-energy correction at two-loop order. Using appropriate assumptions about the form of the inverse of the interacting one-particle Green's function at the FS, we were able to calculate the quasiparticle weight Z, which was shown to vary continuously along the FS. Next, we calculated the RG equations for the coupling functions, taking into account both the leading order term and the feedback of Z into the equations themselves. Although the initial tendency observed in the one-loop analysis of flowing to a strong coupling regime remained, the flows then stopped suddenly at fixed plateau values. Despite that, we emphasized that this was not a clear cut evidence of fixed points in our approach since those values are sensitive to the number of points used in the discretization procedure.

Finally, we proceeded with the calculation of the full two-loop order RG equations for the renormalized coupling functions. In order to do that, we had to calculate also the nonleading divergences which arose from the so-called nonparquet diagrams. As we have seen, their contribution was not cancelled out by the diagrams generated by the counterterms Δg_{1R} and Δg_{2R} defined in one-loop order. That automatically led us to redefine the counterterms which from then on acquired also third-order contributions. For this final case, we chose two different initial conditions to analyze the flows, namely $\overline{g}_{1R} = \overline{g}_{2R} = 10$ and $\overline{g}_{1R} = \overline{g}_{2R} = 1$.

For the first choice of initial conditions, the flows were qualitatively similar to the ones which included the feedback of Z. They were, as a consequence, very dissimilar to the one-loop flow. Afterwards, we numerically analyzed the corresponding flow of the quasiparticle weight as we approached the FS. We observed that Z was anisotropic and strongly suppressed in that limit. We pointed out that Z vanishes faster in the $(\pi, 0)$ or $(0, \pi)$-directions, i.e the center parts of the square FS. Finally, we emphasized that, in view of this strong suppression, there were many coupling functions that renormalized to zero in contrast to the one-loop case where they appeared to increase indefinitely.

In contrast, for the second choice of initial conditions ($\overline{g}_{1R} = \overline{g}_{2R} = 1$), Z changes very mildly from its original unity value. Consequently, the two-loop flows were very similar to the one-loop ones. That is an indication, verified numerically, that the physical state depends directly on the initial choice of coupling strengths. In view of that, we intend to explore further the implications of these results. In addition, we must also analyze how the renormalization of the Fermi velocity and the FS affect our results. This is even more important in view of the recent results obtained by Afchain *et al.*[10] concerning the existence of a Luttinger liquid state in two spatial dimensions. As we already noticed from our self-energy at one-loop order, the Fermi surface and the Fermi velocity are directly affected by interactions. The flows of the FS and v_F to critical regimes naturally impose important new conditions on the flow of the renormalized coupling functions. The coupled RG equations for the renormalized coupling functions, the FS and Fermi velocity should all be solved self-consistently. That naturally places extra difficulties but one should, nevertheless, deal with this problem seriously. We plan to consider those questions in a subsequent publication[20].

Acknowledgments

We wish to acknowledge innumerous discussions with several colleagues during the "RG Methods for Interacting Electrons" Winter School which took place in the ICCMP - UnB, Brasília, during July 12^{th} - August 6^{th}, 2004. We also wish to thank Dionys Baeriswyl and Peter Kopietz for useful comments and suggestions. This work was partially supported by the Financiadora de Estudos e Projetos (FINEP) and by the Conselho Nacional de Desenvolvimento Científico e Tecnológico (CNPq) - Brazil.

APPENDIX A

In this appendix, we will write down the explicit form of the nonparquet contributions which are taken into account in the Eqs. (5.2) and (5.3). We also give the several intervals of integration along the Fermi surface that are considered throughout this work which are the following

$$\mathcal{D}_1 = \left\{ \begin{array}{l} -\Delta \leqslant k_\parallel \leqslant \Delta, \\ -\Delta \leqslant p_{1\parallel} + p_{2\parallel} - k_\parallel \leqslant \Delta. \end{array} \right.$$

$$\mathcal{D}_2 = \left\{ \begin{array}{l} -\Delta \leqslant k_\parallel \leqslant \Delta, \\ -\Delta \leqslant k_\parallel + p_{2\parallel} - p_{3\parallel} \leqslant \Delta. \end{array} \right.$$

$$\mathcal{D}_3 = \left\{ \begin{array}{l} -\Delta \leqslant k_\parallel \leqslant \Delta, \\ -\Delta \leqslant k_\parallel + p_{3\parallel} - p_{1\parallel} \leqslant \Delta. \end{array} \right.$$

$$\mathcal{D}_4 = \left\{ \begin{array}{l} -\Delta \leqslant k_\parallel \leqslant \Delta, \\ -\Delta \leqslant q_\parallel \leqslant \Delta, \\ -\Delta \leqslant p_\parallel \leqslant \Delta, \\ -\Delta \leqslant -k_\parallel + p_\parallel + q_\parallel \leqslant \Delta. \end{array} \right.$$

$$\mathcal{D}_5 = \left\{ \begin{array}{l} -\Delta \leqslant k_\parallel \leqslant \Delta, \\ -\Delta \leqslant q_\parallel \leqslant \Delta, \\ -\Delta \leqslant k_\parallel + q_\parallel - p_{1\parallel} \leqslant \Delta, \\ -\Delta \leqslant k_\parallel + p_{2\parallel} - p_{3\parallel} \leqslant \Delta. \end{array} \right.$$

$$\mathcal{D}_6 = \left\{ \begin{array}{l} -\Delta \leqslant k_\parallel \leqslant \Delta, \\ -\Delta \leqslant q_\parallel \leqslant \Delta, \\ -\Delta \leqslant k_\parallel + q_\parallel - p_{2\parallel} \leqslant \Delta, \\ -\Delta \leqslant k_\parallel + p_{3\parallel} - p_{2\parallel} \leqslant \Delta. \end{array} \right.$$

$$\mathcal{D}_7 = \left\{ \begin{array}{l} -\Delta \leqslant k_\parallel \leqslant \Delta, \\ -\Delta \leqslant q_\parallel \leqslant \Delta, \\ -\Delta \leqslant k_\parallel + q_\parallel - p_{4\parallel} \leqslant \Delta, \\ -\Delta \leqslant k_\parallel + p_{3\parallel} - p_{1\parallel} \leqslant \Delta. \end{array} \right.$$

$$\mathcal{D}_8 = \left\{ \begin{array}{l} -\Delta \leqslant k_\parallel \leqslant \Delta, \\ -\Delta \leqslant q_\parallel \leqslant \Delta, \\ -\Delta \leqslant k_\parallel + q_\parallel - p_{3\parallel} \leqslant \Delta, \\ -\Delta \leqslant k_\parallel + p_{1\parallel} - p_{3\parallel} \leqslant \Delta. \end{array} \right.$$

In addition to that, we must have of course

$$\begin{array}{l} -\Delta \leqslant p_{1\parallel} \leqslant \Delta, \\ -\Delta \leqslant p_{2\parallel} \leqslant \Delta, \\ -\Delta \leqslant p_{3\parallel} \leqslant \Delta, \\ -\Delta \leqslant p_{4\parallel} \leqslant \Delta. \end{array}$$

We begin with the nonparquet diagrams shown in Fig.(7) associated with $\Gamma_1^{(4)}$ we get

$$\begin{aligned} \Delta g_{1R(a)}^{2-loop} &= \frac{1}{32\pi^4 v_F^2} \ln\left(\frac{\Omega}{\omega}\right) \\ &\times \int_{\mathcal{D}_8} dk_\parallel dq_\parallel g_{1R}\left(k_\parallel + p_{1\parallel} - p_{3\parallel}, p_{2\parallel}, k_\parallel\right) \\ &\times g_{1R}\left(p_{1\parallel}, k_\parallel + q_\parallel - p_{3\parallel}, k_\parallel + p_{1\parallel} - p_{3\parallel}\right) \\ &\times g_{2R}\left(k_\parallel, q_\parallel, k_\parallel + q_\parallel - p_{3\parallel}\right), \end{aligned} \tag{A1}$$

$$\begin{aligned} \Delta g_{1R(b)}^{2-loop} &= \frac{1}{32\pi^4 v_F^2} \ln\left(\frac{\Omega}{\omega}\right) \int_{\mathcal{D}_8} dk_\parallel dq_\parallel g_{1R}\left(k_\parallel, q_\parallel, p_{3\parallel}\right) \\ &\times g_{1R}\left(k_\parallel + p_{1\parallel} - p_{3\parallel}, p_{2\parallel}, k_\parallel\right) \\ &\times g_{2R}\left(p_{1\parallel}, k_\parallel + q_\parallel - p_{3\parallel}, q_\parallel\right), \end{aligned} \tag{A2}$$

$$\begin{aligned} \Delta g_{1R(c)}^{2-loop} &= \frac{1}{32\pi^4 v_F^2} \ln\left(\frac{\Omega}{\omega}\right) \int_{\mathcal{D}_7} dk_\parallel dq_\parallel g_{2R}\left(q_\parallel, k_\parallel, p_{4\parallel}\right) \\ &\times g_{1R}\left(p_{1\parallel}, k_\parallel + p_{3\parallel} - p_{1\parallel}, p_{3\parallel}\right) \\ &\times g_{1R}\left(k_\parallel + q_\parallel - p_{4\parallel}, p_{2\parallel}, q_\parallel\right), \end{aligned} \tag{A3}$$

$$\begin{aligned} \Delta g_{1R(d)}^{2-loop} &= \frac{1}{32\pi^4 v_F^2} \ln\left(\frac{\Omega}{\omega}\right) \\ &\times \int_{\mathcal{D}_7} dk_\parallel dq_\parallel g_{1R}\left(p_{1\parallel}, k_\parallel + p_{3\parallel} - p_{1\parallel}, p_{3\parallel}\right) \\ &\times g_{2R}\left(k_\parallel + q_\parallel - p_{4\parallel}, p_{2\parallel}, k_\parallel + p_{3\parallel} - p_{1\parallel}\right) \\ &\times g_{1R}\left(q_\parallel, k_\parallel, k_\parallel + q_\parallel - p_{4\parallel}\right), \end{aligned} \tag{A4}$$

$$\begin{aligned} \Delta g_{1R(e)}^{2-loop} &= -\frac{1}{16\pi^4 v_F^2} \ln\left(\frac{\Omega}{\omega}\right) \\ &\times \int_{\mathcal{D}_8} dk_\parallel dq_\parallel g_{1R}\left(k_\parallel + p_{1\parallel} - p_{3\parallel}, p_{2\parallel}, k_\parallel\right) \\ &\times g_{2R}\left(p_{1\parallel}, k_\parallel + q_\parallel - p_{3\parallel}, q_\parallel\right) \\ &\times g_{2R}\left(k_\parallel, q_\parallel, k_\parallel + q_\parallel - p_{3\parallel}\right), \end{aligned} \tag{A5}$$

and finally

$$\begin{aligned} \Delta g_{1R(f)}^{2-loop} &= -\frac{1}{16\pi^4 v_F^2} \int_{\mathcal{D}_7} dk_\parallel dq_\parallel g_{2R}\left(k_\parallel, q_\parallel, p_{4\parallel}\right) \\ &\times g_{2R}\left(k_\parallel + q_\parallel - p_{4\parallel}, p_{2\parallel}, k_\parallel + p_{3\parallel} - p_{1\parallel}\right) \\ &\times g_{1R}\left(p_{1\parallel}, k_\parallel + p_{3\parallel} - p_{1\parallel}, p_{3\parallel}\right) \ln\left(\frac{\Omega}{\omega}\right), \end{aligned} \tag{A6}$$

using the same conventions for the integrals over momenta components along the Fermi surface as before.

Similarly for the nonparquet diagrams shown in Fig.(8) associated with $\Gamma_2^{(4)}$ we get

$$\Delta g_{2R(a)}^{2-loop} = \frac{1}{32\pi^4 v_F^2}\ln\left(\frac{\Omega}{\omega}\right) \times \int_{\mathcal{D}_5} dk_\parallel dq_\parallel g_{1R}\left(p_{1\parallel}, k_\parallel + q_\parallel - p_{1\parallel}, k_\parallel\right) \times g_{1R}\left(k_\parallel, p_{2\parallel}, k_\parallel + p_{2\parallel} - p_{3\parallel}\right) \times g_{1R}\left(k_\parallel + p_{2\parallel} - p_{3\parallel}, q_\parallel, p_{4\parallel}\right), \quad \text{(A7)}$$

$$\Delta g_{2R(b)}^{2-loop} = \frac{1}{32\pi^4 v_F^2}\int_{\mathcal{D}_6} dk_\parallel dq_\parallel g_{1R}\left(p_{1\parallel}, k_\parallel, p_{4\parallel}\right) \times g_{1R}\left(q_\parallel, k_\parallel + p_{3\parallel} - p_{2\parallel}, k_\parallel + q_\parallel - p_{2\parallel}\right) \times g_{1R}\left(k_\parallel + q_\parallel - p_{2\parallel}, p_{2\parallel}, q_\parallel\right)\ln\left(\frac{\Omega}{\omega}\right), \quad \text{(A8)}$$

$$\Delta g_{2R(c)}^{2-loop} = -\frac{1}{16\pi^4 v_F^2}\int_{\mathcal{D}_5} dk_\parallel dq_\parallel g_{2R}\left(k_\parallel, p_{2\parallel}, p_{3\parallel}\right) \times g_{1R}\left(p_{1\parallel}, k_\parallel + q_\parallel - p_{1\parallel}, k_\parallel\right) \times g_{1R}\left(k_\parallel + p_{2\parallel} - p_{3\parallel}, q_\parallel, p_{4\parallel}\right)\ln\left(\frac{\Omega}{\omega}\right), \quad \text{(A9)}$$

$$\Delta g_{2R(d)}^{2-loop} = -\frac{1}{16\pi^4 v_F^2}\ln\left(\frac{\Omega}{\omega}\right) \times \int_{\mathcal{D}_6} dk_\parallel dq_\parallel g_{2R}\left(p_{1\parallel}, k_\parallel, k_\parallel + p_{3\parallel} - p_{2\parallel}\right) \times g_{1R}\left(q_\parallel, k_\parallel + p_{3\parallel} - p_{2\parallel}, k_\parallel + q_\parallel - p_{2\parallel}\right) \times g_{1R}\left(k_\parallel + q_\parallel - p_{2\parallel}, p_{2\parallel}, q_\parallel\right), \quad \text{(A10)}$$

$$\Delta g_{2R(e)}^{2-loop} = \frac{1}{32\pi^4 v_F^2}\ln\left(\frac{\Omega}{\omega}\right) \times \int_{\mathcal{D}_6} dk_\parallel dq_\parallel g_{2R}\left(p_{1\parallel}, k_\parallel, k_\parallel + p_{3\parallel} - p_{2\parallel}\right) \times g_{1R}\left(q_\parallel, k_\parallel + p_{3\parallel} - p_{2\parallel}, k_\parallel + q_\parallel - p_{2\parallel}\right) \times g_{2R}\left(k_\parallel + q_\parallel - p_{2\parallel}, p_{2\parallel}, k_\parallel\right), \quad \text{(A11)}$$

$$\Delta g_{2R(f)}^{2-loop} = \frac{1}{32\pi^4 v_F^2}\ln\left(\frac{\Omega}{\omega}\right) \times \int_{\mathcal{D}_6} dk_\parallel dq_\parallel g_{2R}\left(p_{1\parallel}, k_\parallel, k_\parallel + p_{3\parallel} - p_{2\parallel}\right) \times g_{1R}\left(k_\parallel + q_\parallel - p_{2\parallel}, p_{2\parallel}, q_\parallel\right) \times g_{2R}\left(q_\parallel, k_\parallel + p_{3\parallel} - p_{2\parallel}, p_{3\parallel}\right), \quad \text{(A12)}$$

$$\Delta g_{2R(g)}^{2-loop} = \frac{1}{32\pi^4 v_F^2}\int_{\mathcal{D}_5} dk_\parallel dq_\parallel g_{2R}\left(k_\parallel, p_{2\parallel}, p_{3\parallel}\right) \times g_{1R}\left(k_\parallel + p_{2\parallel} - p_{3\parallel}, q_\parallel, p_{4\parallel}\right) \times g_{2R}\left(p_{1\parallel}, k_\parallel + q_\parallel - p_{1\parallel}, q_\parallel\right)\ln\left(\frac{\Omega}{\omega}\right), \quad \text{(A13)}$$

$$\Delta g_{2R(h)}^{2-loop} = \frac{1}{32\pi^4 v_F^2}\int_{\mathcal{D}_5} dk_\parallel dq_\parallel g_{2R}\left(k_\parallel, p_{2\parallel}, p_{3\parallel}\right) \times g_{2R}\left(k_\parallel + p_{2\parallel} - p_{3\parallel}, q_\parallel, k_\parallel + q_\parallel - p_{1\parallel}\right) \times g_{1R}\left(p_{1\parallel}, k_\parallel + q_\parallel - p_{1\parallel}, k_\parallel\right)\ln\left(\frac{\Omega}{\omega}\right), \quad \text{(A14)}$$

$$\Delta g_{2R(i)}^{2-loop} = -\frac{1}{16\pi^4 v_F^2}\ln\left(\frac{\Omega}{\omega}\right) \times \int_{\mathcal{D}_6} dk_\parallel dq_\parallel g_{2R}\left(p_{1\parallel}, k_\parallel, k_\parallel + p_{3\parallel} - p_{2\parallel}\right) \times g_{2R}\left(k_\parallel + q_\parallel - p_{2\parallel}, p_{2\parallel}, k_\parallel\right) \times g_{2R}\left(q_\parallel, k_\parallel + p_{3\parallel} - p_{2\parallel}, p_{3\parallel}\right), \quad \text{(A15)}$$

and finally

$$\Delta g_{2R(j)}^{2-loop} = -\frac{1}{16\pi^4 v_F^2}\int_{\mathcal{D}_5} dk_\parallel dq_\parallel g_{2R}\left(k_\parallel, p_{2\parallel}, p_{3\parallel}\right) \times g_{2R}\left(k_\parallel + p_{2\parallel} - p_{3\parallel}, q_\parallel, k_\parallel + q_\parallel - p_{1\parallel}\right) \times g_{2R}\left(p_{1\parallel}, k_\parallel + q_\parallel - p_{1\parallel}, q_\parallel\right)\ln\left(\frac{\Omega}{\omega}\right). \quad \text{(A16)}$$

APPENDIX B

In this appendix, we explain briefly how the cancellation of the $\ln^2(\Omega/\omega)$ contributions takes place in two-loop order within our scheme. In higher-loop orders, only the cancellations of the leading divergence are guaranteed by the existing one-loop counterterms. However, we saw that in two-loop order there were also new diagrams associated with nonleading logarithmic divergence, which

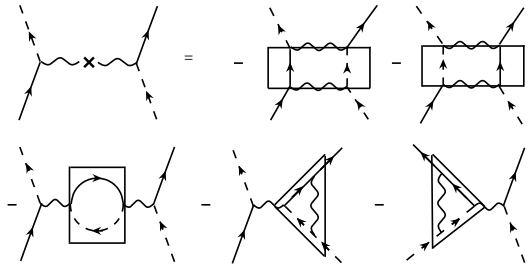

FIG. 18: The counterterm diagrams of Δg_{1R} up to one-loop order displayed in terms of constituent blocks.

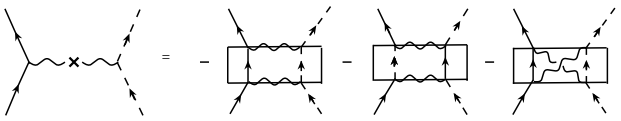

FIG. 19: The counterterm diagrams of Δg_{2R} up to one-loop order displayed in terms of constituent blocks.

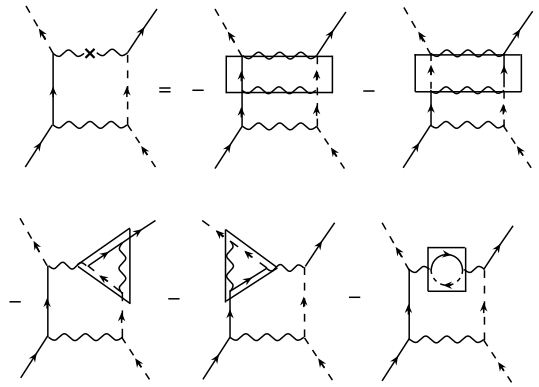

FIG. 20: A two-loop example with Δg_{1R} mixed with the usual interaction vertices.

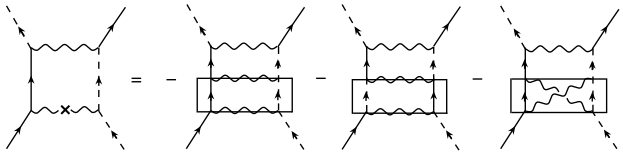

FIG. 21: A two-loop example with Δg_{2R} mixed with the usual interaction vertices.

were not accounted by the one-loop order counterterms. This led us to redefine Δg_{1R} and Δg_{2R} in two-loop order. This is consistent with the fact that we do not know, *a priori*, the exact expression for the counterterms and, for this reason, they must be calculated order by order in perturbation theory.

Firstly, recall Eq.(5.1), in which the Lagrangian is written in terms of the renormalized parameters of the theory together with the corresponding counterterms. Since every term in the interacting part of the Lagrangian generates Feynman diagrams in perturbation theory, so do the counterterms in our case.

To illustrate our argument, the counterterms in one-loop order for Δg_{1R}^{1-loop} and Δg_{2R}^{1-loop} are now displayed graphically in terms of constituent blocks in Figs.18 and 19. In this way, when we go to higher orders, Feynman diagrams are generated, in which these blocks mix with the usual interaction vertices. This will produce the expected cancellations of the leading divergence in that order of perturbation. As an example, consider the diagrams of Figs.20 and 21. Since the Δg_{1R}^{1-loop} and Δg_{2R}^{1-loop} are logarithmically divergent on their own, when they are inserted in a logarithmically divergent bubble, they produce a $\ln^2(\Omega/\omega)$ contribution. This cancels exactly the leading order divergence produced by conventional perturbation theory. However, in order to avoid double-counting of these counterterms contributions, we need to take into account the various symmetry relations which exist among diagrams constructed with some of the counterterms blocks. We illustrate one of these symmetry relations in Fig.22. Following this, only the single logarithmic divergences from the nonparquet diagrams are left out of these cancellation processes and they are used to redefine Δg_{1R} and Δg_{2R} in two-loop order.

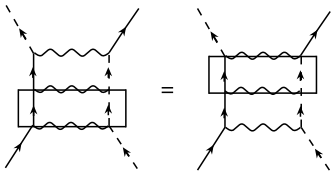

FIG. 22: A symmetry relation example of diagrams generated by different constituent blocks.

[1] P.W. Anderson, Science **235**, 1196 (1987).

[2] See, e.g., J. C. Campuzano, M. R. Norman and M. Randeria, *in Physics of Conventional and Unconventional Superconductors*, edited by K. H. Bennemann and J. B. Ketterson, Springer-Verlag (2003).

[3] D. S. Dessau, Z. -X. Shen, D. M. King, D. S. Marshall, L. W. Lombardo, P. H. Dickinson, A. G. Loeser, J. DiCarlo, C. -H. Park, A. Kapitulnik and W. E. Spicer, Phys. Rev. Lett. **71**, 2781 (1993).

[4] T. Yoshida, X. J. Zhou, T. Sasagawa, W. L. Yang, P. V. Bogdanov, A. Lanzara, Z Hussain, T. Mizokawa, A. Fujimori, H. Eisaki, Z. -X. Shen, T. Kakeshita and S. Uchida, Phys. Rev. Lett. **91**, 27001 (2003).

[5] A. Virosztek and J. Ruvalds, Phys. Rev B **42**, 4064 (1990).

[6] A. T. Zheleznyak, V. M. Yakovenko and I. E. Dzyaloshinskii, Phys. Rev B **55**, 3200 (1997).

[7] F. V. Abreu and B. Douçot, Europhys. Lett. **38**, 533 (1997).

[8] A. Luther, Phys. Rev. B **50**, 11446 (1994).

[9] J. O. Fjaerestad, A. Sudbo and A. Luther, Phys. Rev. B **60**, 13361 (1999).

[10] S. Afchain, J. Magnen and V. Rivasseau, arXiv:cond-mat/0409231 (2004).

[11] M. Abrecht, D. Ariosa, D. Clotta, S. Mitrovic, M. Onellion, X. X. Xi, G. Margaritondo and D. Pavuna, Phys. Rev. Lett. **91**, 57002 (2003).

[12] C. Honerkamp and M. Salmhofer, Phys. Rev. B **67**, 174504 (2003).

[13] A. A. Katanin and A. P. Kampf, Phys. Rev. Lett. **93**, 106406 (2004).

[14] J. Solyom, Adv. Phys. **28**, 202 (1979).

[15] A. Ferraz, Phys. Rev B **68**, 75115 (2003).

[16] A. Ferraz, Europhys. Lett. **61**, 228 (2003).
[17] M. Peskin and D. M. Schroeder, *An Introduction to Quantum Field Theory*, (Perseus Books, 1995).
[18] P. Kopietz and T. Busche, Phys. Rev. B **64**, 155101 (2001).
[19] J. I. Kishine and K. Yonemitsu, Phys. Rev. B **59**, 14823 (1999).
[20] H. Freire, E. Corrêa and A. Ferraz (unpublished).